90-Inch Prime Focus Corrector

L e n s 3 T e s t i n g R e p o r t

Michael Tuell - *Optical Sciences Center, University of Arizona, Tucson, Arizona 85716*

June 1, 2001

Abstract

This report details the test methods and results for lens 3 of the 90PFC system. It was found to meet specifications in a transmission test configuration.

Table of Contents

Summary

Lens 3 for the 90PFC is a 10.25” diameter plano-convex lens made of fused silica. It was tested in double-pass transmission mode with a flat return mirror, meaning that the lens acted as a collimator. The lens is not designed to be a collimator in its final configuration, which means that we were not using it at the correct conjugates, which introduced spherical aberration. To correct for this, a two-element negative lens was introduced into the system to compensate for this inherent spherical aberration. Figure 1 shows the test system layout. The distance from the interferometer focus (at the right side of the figure) to the vertex of the test lens was 1.175 meters. An f/3.3 transmission sphere was used as the reference in the interferometer.

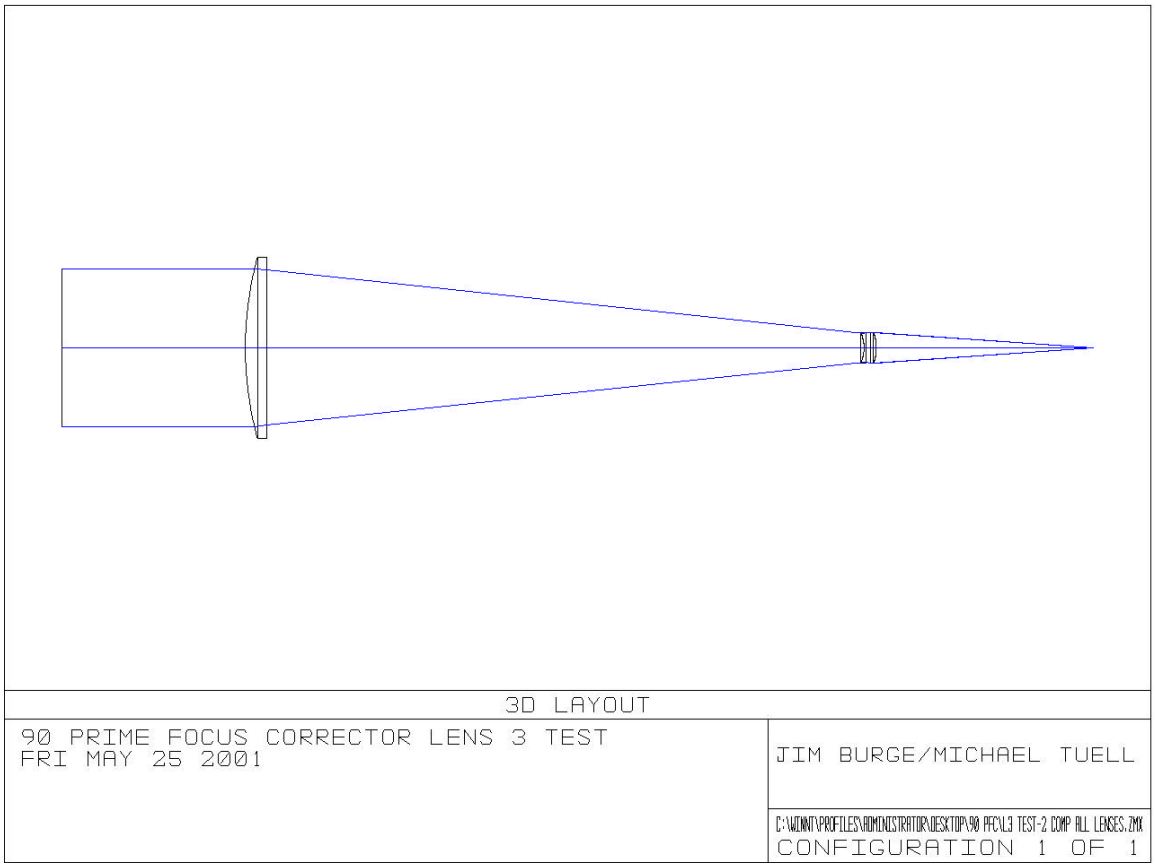

Figure 1

A laser-based Fizeau phase-stepping interferometer was used at 632.8 nm. Due to mounting constraints, this setup only allowed us to only test 90% of the total clear.

After careful alignment, there was residual coma and astigmatism in the test setup. Coma was removed by translating the test lens laterally. Astigmatism remained in the system, so four measurements were taken with the test lens rotated 90° between measurements. These measurements were then averaged to remove systemic astigmatism

and residual coma. After this averaging was performed, a phase map was obtained with an rms value of 0.0217 waves. System tolerance analysis of the Prime Focus Corrector (PFC) showed that the performance goal was on the order of 0.08 waves rms, so the lens exceeds specifications by a factor of four. Figure 2 shows the final phase map. Note the 4-theta term which is present. Chances are good that this is also in the test optics – not in lens 3. If the lens were rotated to five positions instead of four, this would have more than likely also been averaged out.

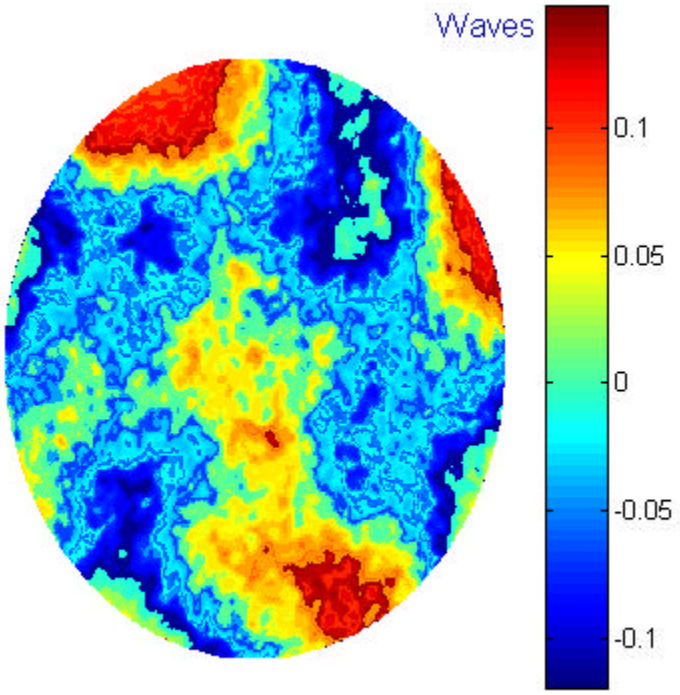

Figure 2

Bottom line: lens 3 meets its specifications in transmission.

A second measurement performed was the difference between the mechanical axis and optical axis. This turned out to be 1.30 ± 0.05 mil (0.0013”), or equivalently, 0.018 mm of wedge.

Appendix A: System vs. Lens Tolerances

By inspecting the system tolerances and comparing them to the tolerances of lens 3, we can find an average ratio, which relates rms spot size to rms wavefront. Table A1 relates the physical parameters of lens 3 to rms spot radius.

System Parameter	RMS spot radius (mm)
Radius 1	0.000270
Surface 1	0.001138
Thickness	0.000100
Flatness	0.000100
Surface 2	0.001138
Wedge	0.000400
Tilt	0.001050
Decenter	0.000680
Index	0.000050
Index homogeneity	0.000218
Root Sum Square total	**0.0017009**

Table A1

The PFC specifications are given in terms of rms spot radius, whereas the lens measurements are in terms of wavefront. A conversion between these is possible by looking at the rms spot radius and rms wavefront vs. field in Zemax.

Comparing the rms spot radius vs. field to the rms wavefront vs. field for the complete system, we can approximate a ratio of 15 to 20 microns of spot radius per wave of wavefront. The value of 20 microns per wave was used. Dividing 1.7009 microns by 20 microns per wave gives a wavefront error tolerance of 0.0850 waves rms. Figure A1 shows the field dependence of rms spot radius and wavefront.

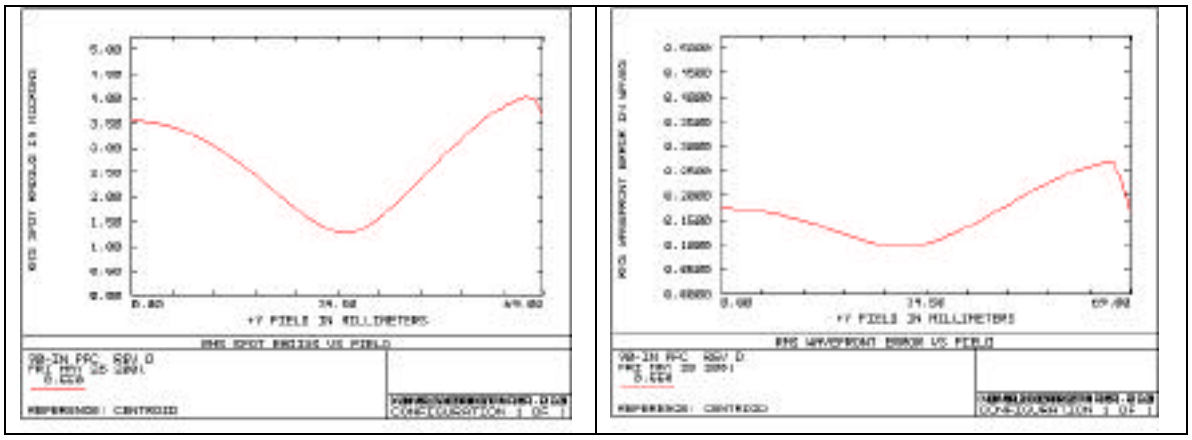

Figure A1

Appendix B: Testing System Tolerance Analysis

In order to model the opto-mechanical tolerances for the test system, Zemax was used to individually perturb system element locations. The rms wavefront changes from each perturbation were then added together by the root sum square method. Each part of the system was carefully measured and the measurement tolerance was used to perturb the system. For example: the radius of curvature, center thickness and wedge of each of the two auxiliary lenses was measured. The measured values were then used in the Zemax model instead of the values specified in the catalog to improve the model. Each measurement has some error in it – these measurement tolerances were estimated and then the model was perturbed by this amount. For example: the radius of curvature of the first small lens was measured to be 64.64 mm with an uncertainty of 0.02 mm. First, the model was changed to 64.66 mm and optimized, then, it was changed to 64.62 mm and re-optimized.

To optimize the system in Zemax, the merit function defines the real lateral ray height to be zero at the focus of the interferometer, with further constraints on the best wavefront. The location of focus was given much more weight than the wavefront shape. To optimize a system, there must be variables for Zemax to change. In this case, the variables were the following items: the longitudinal position of lens 3 (for focus control), the lateral position of lens 3 (for minimizing coma), and the tip/tilt of the return flat.

Even with no perturbations in the system, it was still not perfect. In fact, the rms wavefront error was 0.010420 waves. To find the additional rms error introduced by perturbation of a system element, we need to take the rms error reported squared minus the square of the unperturbed rms error and then take the square root of that. This is simply root sum square in reverse.

Table B1 shows the rms error and change from the unperturbed case for each system parameter. All of the perturbations are “as measured” values of alignment tolerances. Each system parameter can only be measured/aligned to within a certain tolerance. These values are those tolerances for the specific metrology or alignment technique used. Each parameter was calculated for both “+” and “–“ directions. If the two errors were different, only the largest one is reported.

Figure B1 is a bar chart showing the relative increase for each perturbation (in rms waves.) The x-axis is the index number listed in Table B1. In all cases, the larger of the two rms errors (either “+” the tolerance or “–“ the tolerance) was chosen for the graph and included in the root sum square calculation of the total error budget.

By taking the root sum square of the additional rms values, we find a total of 0.01606 waves rms. This value is well below the target tolerance of 0.0850 waves rms, which means that if these tolerances are held, the data obtained will be useful in determining if the test lens is within its tolerance budget.

Lens 3 Test System Tolerance Table

Element	Index		RMS (waves)	Additional RMS
		Unperturbed	0.010420	0.0000000
Lens placement	1	Z +0.125 mm	0.015109	0.0109410
KPX190	2	R +0.02 mm	0.010818	0.0029074
	3	Tc +0.02 mm	0.010884	0.0031441
	4	Wedge +0.03°	0.010997	0.0035153
	5	Y +0.005 mm	0.010431	0.0004789
	6	Theta x +0.003°	0.010422	0.0002042
Lens spacing	7	T + 0.05 mm	0.013487	0.0085629
KPC076	8	R +0.02 mm	0.011008	0.0035496
	9	Tc +0.02 mm	0.010884	0.0031441
	10	Wedge +0.01°	0.010453	0.0008299
	11	Y +0.025 mm	0.010680	0.0023422
	12	Theta x +0.03°	0.010611	0.0020042
LENS 3	13	Theta x +0.02°	0.010426	0.0003537
Both small Lenses Together	14	Y + 0.2 mm	0.010459	0.0009024
	15	Theta x + 0.1°	0.010441	0.0006619
Root Sum Square				**0.01606**

Table B1

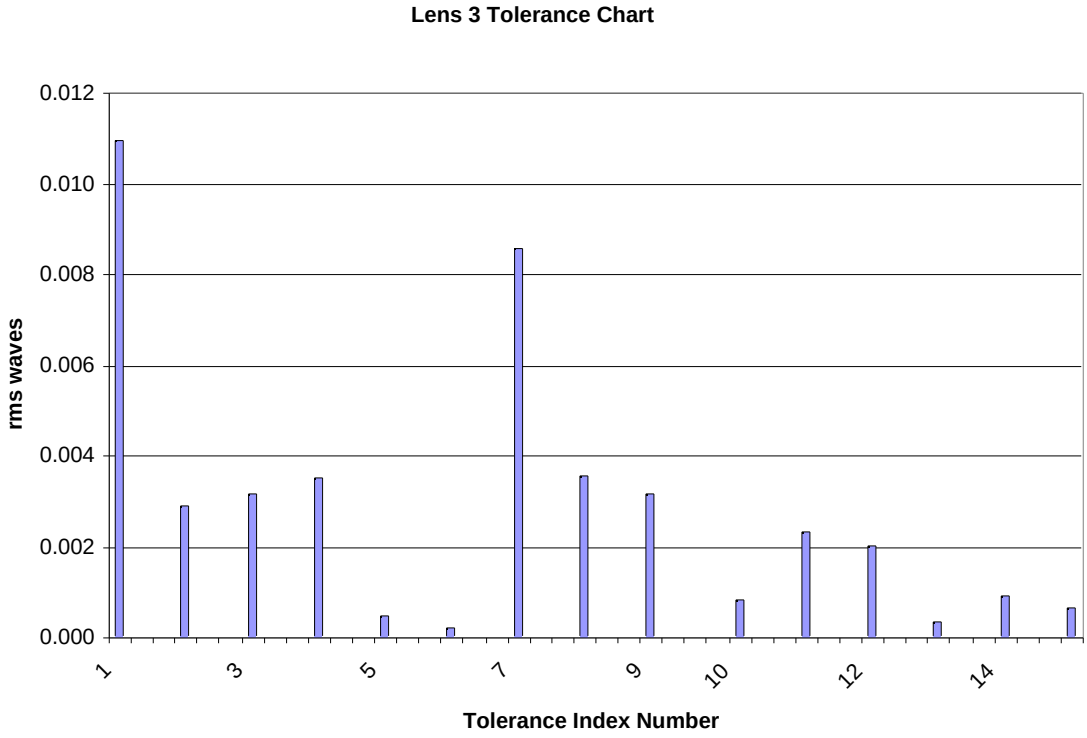

Figure B1

Measurements

For the two small lenses (KPX190 and KPC076 from Newport), the radii of curvature were measured with an interferometer and a radius slide. The beam was focused on the lens surface, and the distance to where the radius of the wavefront matched the radius of the surface was measured. These measurements were accurate to about 0.02 mm. The center thickness was measured on a flat surface with a digital dial indicator that has a resolution of 50 millionths of an inch. It was difficult to measure it that accurately, however, so the true tolerance was again around 0.02 mm. To measure the wedge in the lenses they were again placed on a flat with a digital indicator. They were placed on the flat surface such that the edge of the optic was touching a v-block in two locations, then the optic was rotated. This ensures the mechanical center of rotation is found and a wedge angle can then be determined. The KPX190 was measured to have about 0.03° wedge, and the KPC076 has about 0.01° wedge.

The longitudinal placement of the two lenses was measured by placing one face of an inside micrometer at the focus of the interferometer and carefully moving the two lenses forward until the vertex of the first lens barely touched the other face of the micrometer. The distance between faces of the inside micrometer was measured with an outside micrometer. An estimate for the accuracy of the lens placement is 0.005”.

The distance between the two small lenses was measured with a micrometer with an estimated accuracy of 0.002". Further information about this alignment is given in Appendix C.

The decentration between the two small lenses was measured on an air bearing table with two dial indicators to measure the difference in sag as the surfaces rotated about the air bearing axis. These measurements were done at a radius of about a half inch. Figure B2 tells us that KPX190 is about 4 microns from center and KPC076 is about 25 microns from center.

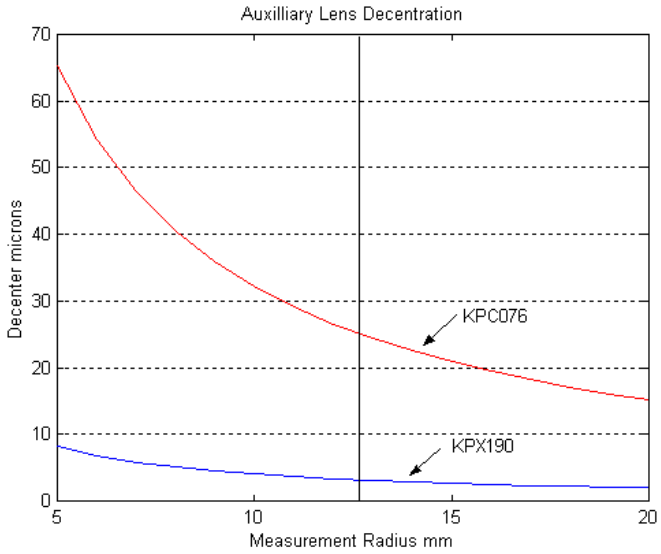

Figure B2

Since these surfaces are spherical, there is no real difference between decentration and tilt. Figure B2 is a calculated plot of decentration, but the same axial runout can be related to surface tilt by simple geometry. In reality, only one of these errors is necessary, but Table B1 lists both. The effect is relatively small, however (indices 5/6 and 11/12), so it does not affect our tolerance budget to include it both ways.

The tilt of lens 3 has a stated tolerance of 0.02°. This was maintained by reflecting a laser beam from the plano surface and observing the displacement of the reflected spot. The geometry of this test is such that with a displacement of 0.1", the angular change is about 0.023°. Displacements of 0.1" are easily detectable by eye.

To determine the tolerances for both small lenses together, simple geometry was employed for calculating the tilt. The two flat surfaces were around 310 mm from the focus and the return reflection could be centered to within 1 mm, so the tilt can be determined to within 0.1°. The tolerance for centering the two spherical surfaces was determined by actually moving the lenses around and estimating how well the (larger) reflected spot could be centered. The worst-case scenario was 0.2 mm, but the actual alignment was better than that.

Appendix C: Testing System Alignment Procedures

Alignment of the test system was a multiple step operation. The first thing to do was to align the two small lenses together. These lenses are standard Newport 2" diameter lenses. One of the lenses is plano-convex, and the other is plano-concave. The two flat surfaces face each other, separated by a little over 6 mm. A 2" barrel I.D. was not available that was long enough, so two individual stock Newport lens mounts were employed. Examination of the mounts revealed that the surfaces were not flat and the spacing from the lens surface plane to the outside of the housing was not constant. To fix these problems, the anodized aluminum mounts were carefully lapped on a steel plate with 40-micron aluminum oxide grinding compound. First, the side adjacent to the plano surface was lapped to flatten the surface. This also removed the wedge between the inside of the retaining ring and the outside of the housing. This was done to about 0.001" around the perimeter. Next, the back surface was lapped to flatten the surface and remove wedge between the two outside surfaces of the mount.

This procedure was done for both mounting cells. The lenses were placed into their cells and the distance from the optical plano surface to the outside of the cells was measured. These distances were subtracted from the overall distance between lenses. This left us with the required thickness of the spacer. An aluminum ring was lapped flat with no wedge between surfaces to the desired thickness of 0.1195". This ring was attached with epoxy from the edge (so we maintain metal-to-metal contact) to one of the lens mounts.

The two lenses were inserted into their cells with a plastic retaining ring holding them in. The plano-concave lens (KPC076) was placed on an air-bearing table with a central hole with the concave side down. A dial indicator with a Teflon tip was placed on the curved surface. The lens was positioned on the table such that the axial runout was minimized (a 0.0005" maximum runout was observed). This defined an optical axis nearly coincident with the mechanical axis of the air-bearing table. The table was tilted such that the flat side had a runout on the same order as the wedge measured in the lens.

The second lens cell was placed on top of the first cell, with the convex side up. A second dial indicator was placed above the first one on the surface of KPX190. The second lens was carefully positioned to minimize the axial runout. On the digital dial indicator, the runout was minimized to the 0.00005" resolution of the indicator. Figure B2 shows the dependence of axial runout on lateral optical axis position for both lenses.

The two cells were then carefully epoxied together at the edge to make a single component. This was then placed in a three-jaw chuck with built-in tip/tilt adjustments. This mount was then placed on a 3-axis translation stage, giving a total of five degrees of freedom for the two-lens combination. See Figure D5 for a picture of this sub-system.

Mounting the test lens (lens 3) was done in a gimble mount with an inside diameter of 12.5". Three plastic blocks were machined with a groove in each one to accept the edge of the lens. A small plastic-tipped setscrew was used to keep the lens

steady. These blocks were placed 120° apart in the gimble mount, and the lens placed in the blocks. The gimble has built-in tip/tilt adjustments and an external vertical translation stage. This entire mount was placed on a two-axis translation stage, so the lens had five degrees of freedom.

The return flat was 24" in diameter and spray silvered. It was mounted in a dual chain mount with safeties on the front and back at the bottom, which allowed for vertical tipping. Tilting the flat to minimize tilt fringes in the horizontal direction was a challenge, but was done by hand by moving it slightly in the chains. See Figure D6 for a picture of the return flat and lens 3.

The interferometer itself was on a vertical translation stage to allow fine adjustment of optical axis height. The axis was about 14 inches from the surface of the floating optical table.

After getting the two lenses together and very rough placement of the several elements, the first thing done was to find the "natural" axis of the interferometer. Any ray going through focus could be defined as the axis, however, to center the image on the CCD array, we want to use the center of the beam if possible. To find the central ray, we first placed f/3.3 transmission sphere into the bayonet mount and tilted it to center the reflected spot on the crosshairs of the Zygo interferometer in "align" mode. Once that was accomplished, a plastic card with a small hole in it is placed such that the focused spot was centered in the hole. This hole then roughly defines our focal point. Removing the transmission sphere gives a collimated beam – part of which goes through the hole in the card. This beam is fairly weak, but it can be seen with the lights dimmed.

This collimated beam is used to roughly center the two-lens combination and test lens. This is not done with any great precision; it merely helps us to keep our interferograms centered on the CCD.

An external laser was set up with two fold flats to align the beam through the hole and through the center of the two-lens combination. The beam was blocked after the two lenses to remove stray reflections. Because there are two lenses (four surfaces), we see four reflected spots. In actuality, we only saw two spots with interference fringes in them because the alignment was good. See Figures D1 and D2.

To adjust the tip/tilt of the two lenses we looked at the (smaller) beam reflected from the two flat surfaces. Adjusting the tip/tilt, we can center the reflected spot back onto the hole in the card. By adjusting the lateral directions, we were getting the vertices of the curved surfaces aligned. This reflected spot is larger because of the curvature. Moving the lenses in x-y slightly alters the spots reflected from the flat surfaces, so this process is iterative. Once all four spots are centered on the hole, we didn't adjust these elements again. See Figure D4 to see the reflected beams.

To get the lenses positioned axially, we used an inside micrometer set to the correct distance from the focal point. Observing the interferogram of the reflected beam,

we looked for straight fringes, signifying that we were at the focus. We then carefully moved the lenses forward with a translation stage until the vertex of the convex surface just touched the other side of the inside micrometer. All adjustments of the two small lenses were then completed, and the elements were not adjusted again. See Figure D3.

The beam block was moved from in front of lens 3 to behind it so we could see reflections from the test lens. Again, the tip/tilt was adjusted by looking at the reflection from the flat (first) surface and lateral position was adjusted by looking at the reflection from the curved (second) surface. Both beams were adjusted to be centered on the hole in the card. The beam block was then removed and the beam from the return flat is adjusted to be at the hole also. See Figures D7 and D8 for the full system layout.

At this point, the fold flat is removed and the transmission sphere is replaced and re-aligned. We obtained fringes with small adjustments of the return flat. A piece of paper was placed in the beam near the test lens so the interferometer could be focused at that location for best results.

Initially, there was defocus, coma and astigmatism in the beam, along with a small amount of third-order spherical aberration. The spherical could come from incorrect spacing or positioning of the two small lenses, or it could be in the test lens itself. Therefore, no adjustment was made to alter the spherical aberration. Misalignment of the two small lenses introduces coma and astigmatism in the wavefront. The Zemax model included a way to minimize the coma by lateral translation of the test lens. Defocus is adjusted by longitudinal adjustment of the test lens.

By acquiring five interferograms and unwrapping the phase map with IntelliWave, we were able to calculate the Zernike coefficients. First, the focus was minimized to around 0.03 waves by translating the test lens longitudinally. By moving it slightly and taking another data set, the Zernike coefficient for focus was altered until it was near zero. Subsequent data sets removed both tilt and focus from the data automatically. Coma was minimized in a similar fashion. By taking a data set and looking at the x and y coma coefficients, we were able to translate the test lens laterally in x-y to minimize the coma to under 0.05 waves in each direction.

Appendix D: Test Results

After removing the coma, astigmatism still remained (about 0.5 waves.) Figure D1 shows an individual phase map, clearly showing the astigmatism.

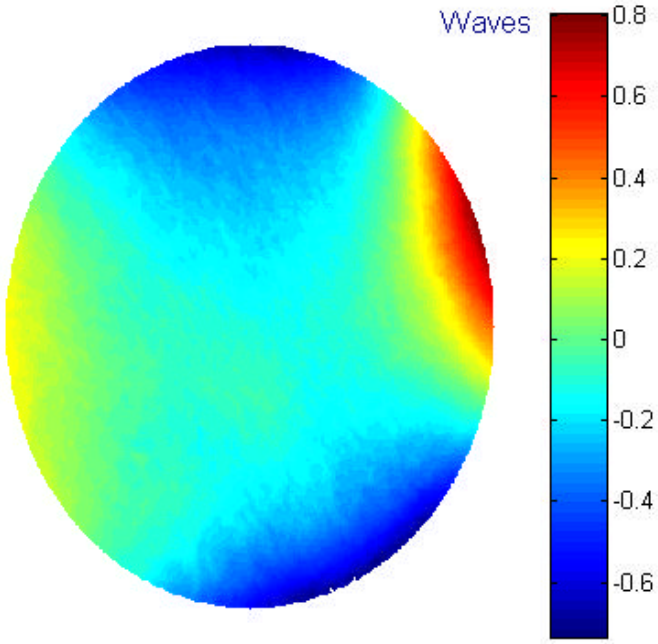

Figure D1

First, we verified that the astigmatism was in the test system, not in lens 3. This was done by rotating lens 3 and observing that the astigmatism axis did not rotate also. Having done this, we decided to subtract systemic astigmatism by rotating the test lens to four discrete positions separated by 90°.

At each rotation point, we took three phase maps and averaged them together to reduce noise. Also, 7x7 median filtering was applied to the averaged phase map to further reduce high-frequency components that should not be in the test lens. These smoothed maps were then combined. Each map was rotated by the amount that the lens was rotated for that particular measurement. That oriented each map so the lens is in the same position in each one. The astigmatism rotated when we did this operation, of course. By averaging all four rotated maps, any aberration that is in the test system (not in the test lens), which has an angular dependency of 3-theta or less, will be subtracted out.

After performing this data manipulation, the phase map in Figure 2, was obtained. It has a peak-to-valley range of 0.268 waves and an rms of 0.0217 waves. The difference between optical and mechanical axes was determined by rotating the lens in a rigid "square" and measuring the axial runout near the edge of the lens. The axial runout was 0.0007", which translates to 0.0013" of lateral displacement between the optical axis and the mechanical axis. This also translates to 0.018 mm of wedge.

Appendix D: Testing System Photographs

Figure D1 Two fold flats and card with hole.

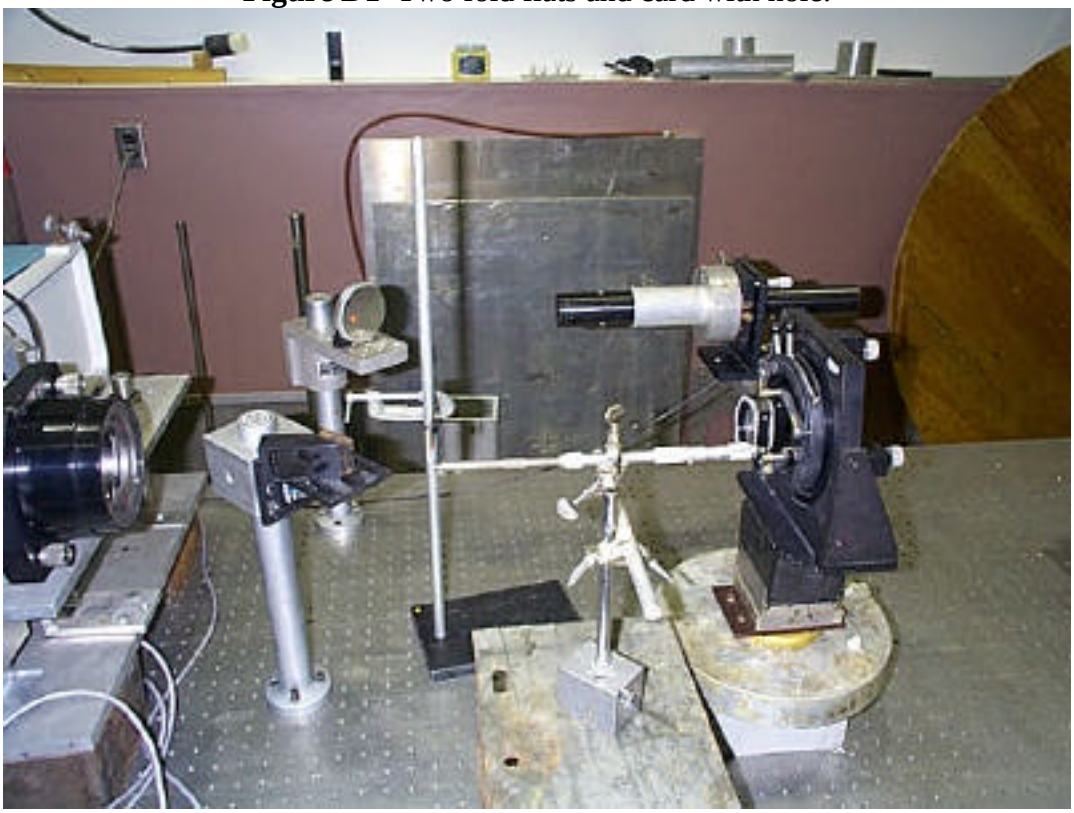

Figure D2 Front-end setup

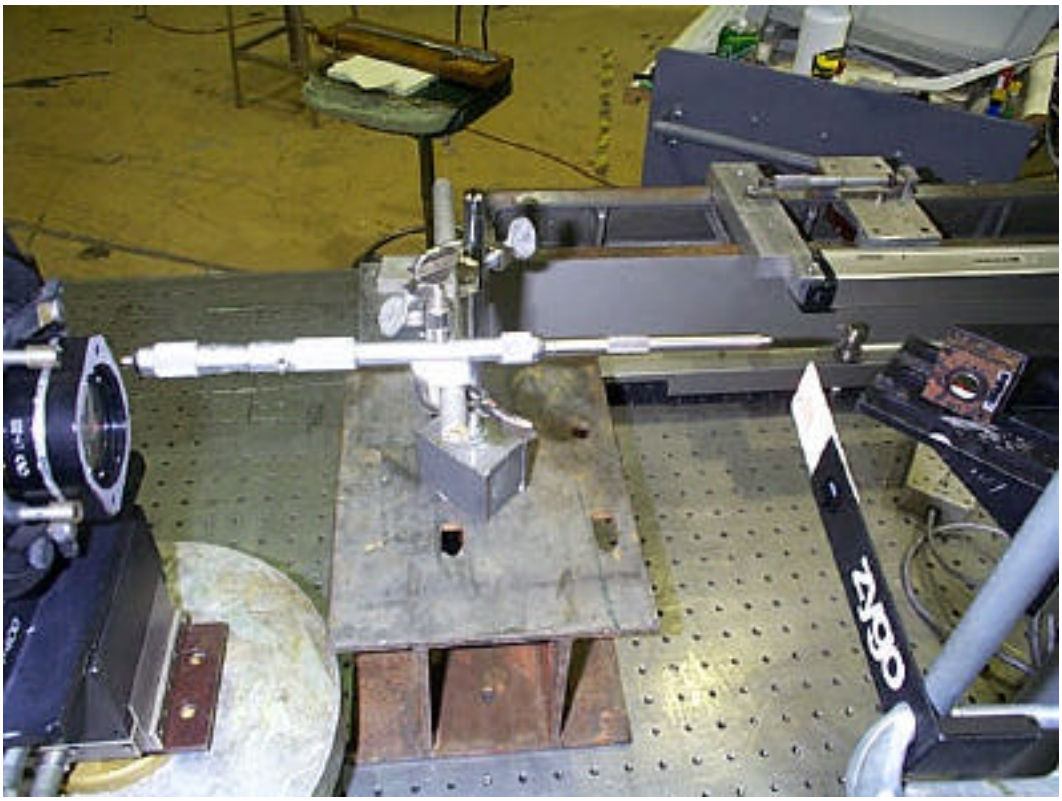

Figure D3 Inside micrometer prior to alignment

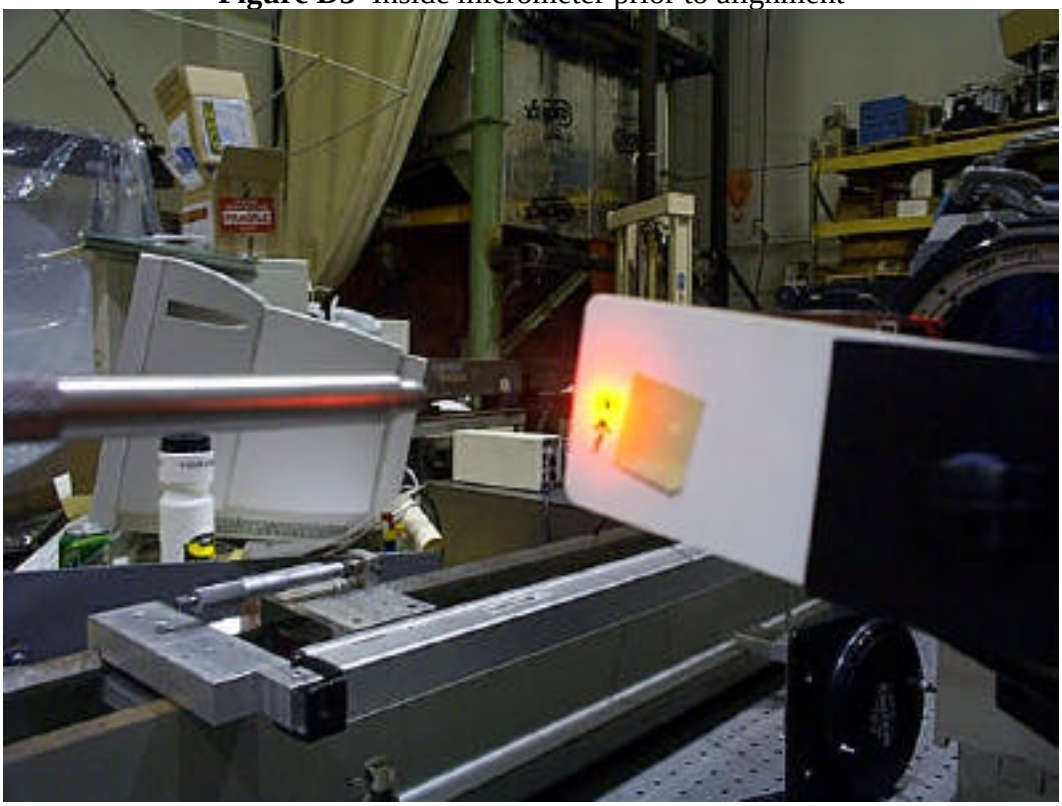

Figure D4 Laser beam reflections nearly centered on hole

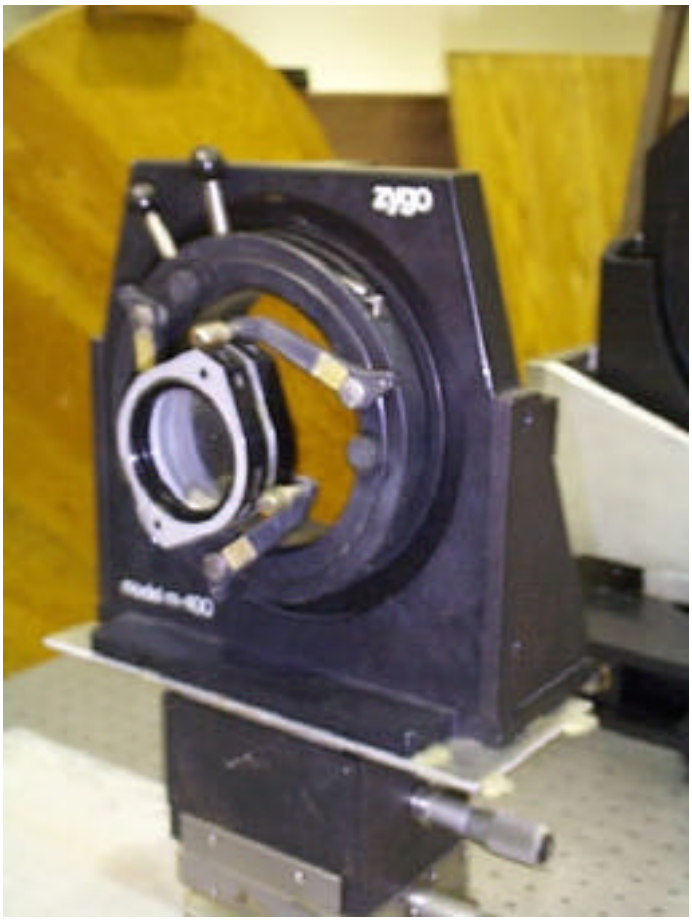

Figure D5 Auxiliary lenses mounted on 5-axis stage

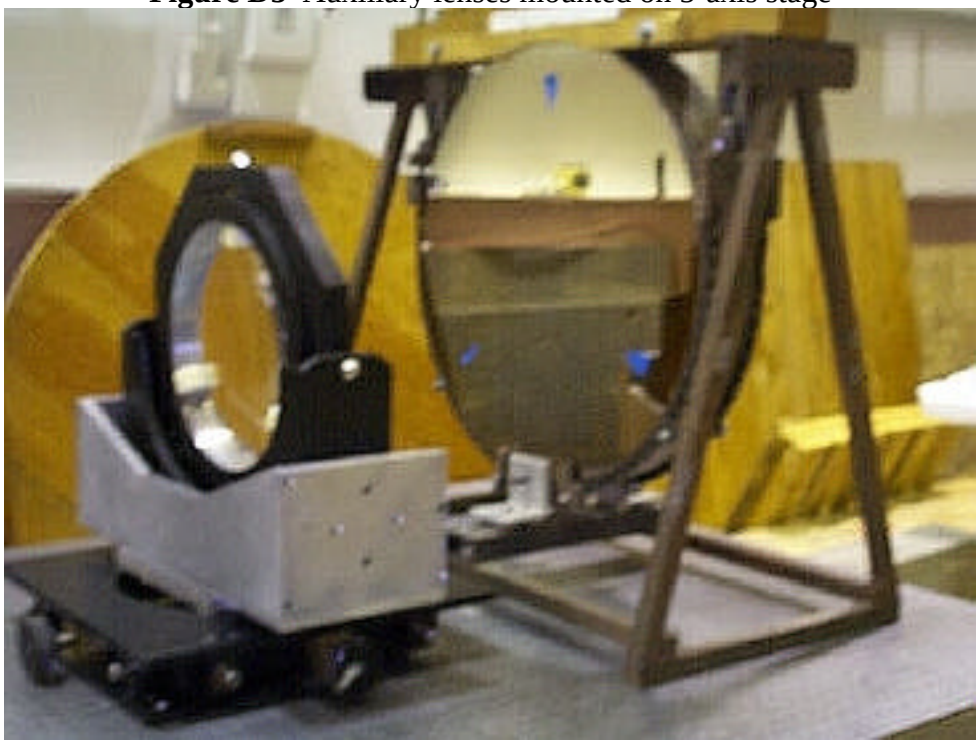

Figure D6 Lens 3 in 5-axis mount and return flat

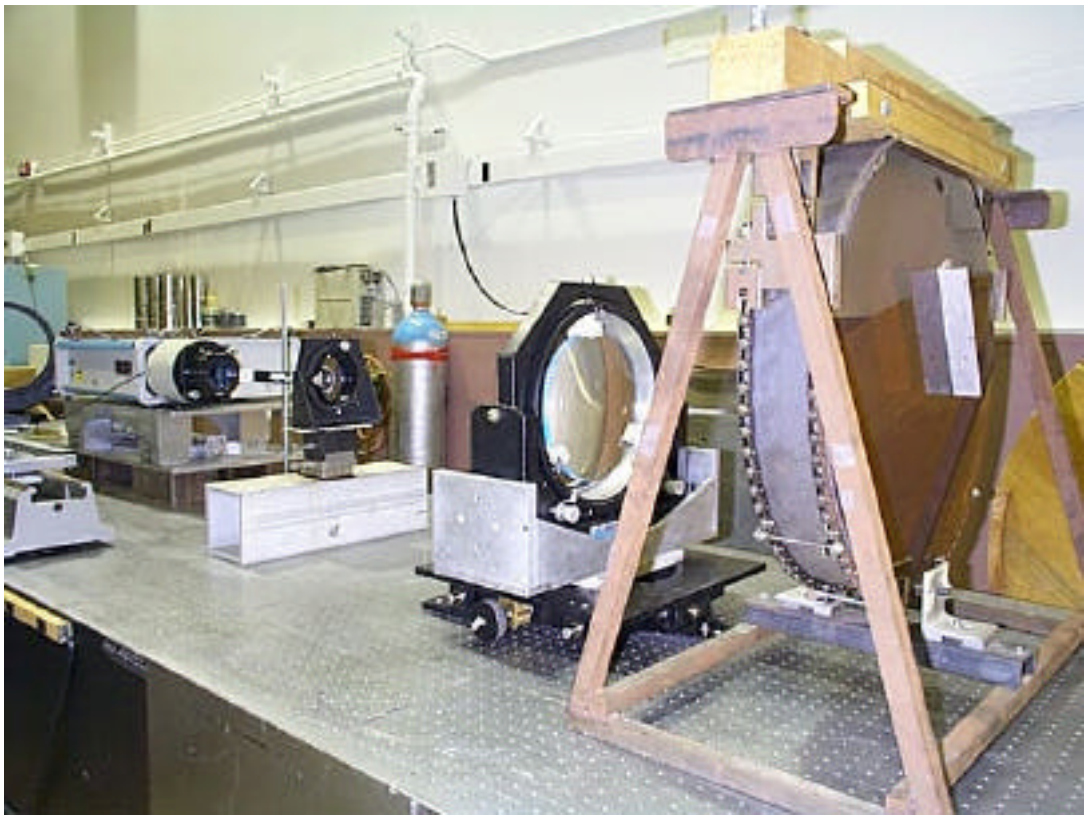

Figure D7 Test system as seen from return flat

Figure D8 Test system as seen from interferometer

Appendix E: Testing System Zemax Analysis

The test system was modeled in Zemax in a double-pass configuration at 633 nm. Appropriate coordinate breaks were inserted to allow perturbations for tolerancing, as detailed in Appendix B.

The optimized (unperturbed) system did not have a perfect wavefront. The rms error was reported as 0.010420 waves. Figure E1 shows the OPD as calculated for the unperturbed system. It has a peak-to-valley error of about 0.05 waves.

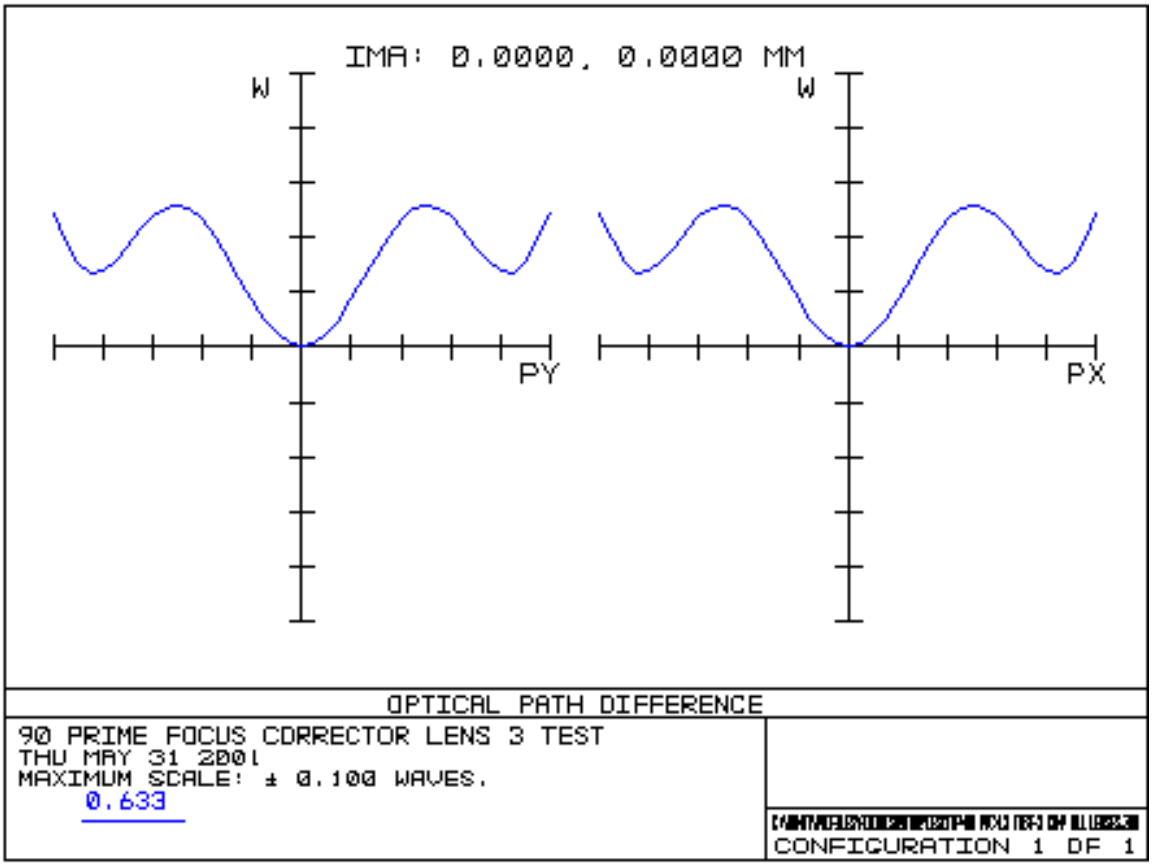

Figure E1

Table E1, below, shows the full double-pass test system including coordinate breaks for each lens and the return flat. A separate file was created to model wedge and decenter for each optical surface of the two smaller lenses.

Test System Prescription

Surf	Type	Comment	Radius	Thickness	Glass	Diam.	Conic
OBJ	STANDARD		Infinity	-300.5519		0	0
1	STANDARD	FOCUS 2 LENSES	Infinity	0		0	0
2	COORDBRK		-	0		-	-
STO	STANDARD	KPX190	-64.64	-8.34	BK7	42.92	0
4	STANDARD		Infinity	0		42.92	0
5	COORDBRK		-	-6.054709		-	-
6	COORDBRK		-	0		-	-
7	STANDARD	KPC076	Infinity	-2.62	BK7	42.92	0
8	STANDARD		-51.65	0		42.92	0
9	STANDARD		Infinity	0		0	0
10	COORDBRK		-	-827.3694		-	-
11	STANDARD	FOCUS ADJUST	Infinity	0.0001677368		0	0
12	COORDBRK	MOVE LENS	-	0		-	-
13	STANDARD	LENS 3	Infinity	-30.21	SILICA	240	0
14	STANDARD		478.59	0		240	0
15	COORDBRK	UNMOVE LENS	-	-254		-	-
16	STANDARD		Infinity	-0.0001677368		0	0
17	COORDBRK	TILT MIRROR	-	0		-	-
18	STANDARD	RETURN FLAT	Infinity	0	MIRROR	218.28	0
19	COORDBRK	UNTILT MIRROR	-	254		-	-
20	STANDARD		Infinity	0.0001677368		0	0
21	COORDBRK	PICKUP 13	-	0		-	-
22	STANDARD	LENS 3	478.59	30.21	SILICA	240	0
23	STANDARD		Infinity	0		240	0
24	COORDBRK	PICKUP 10	-	827.3694		-	-
25	STANDARD		Infinity	0		0	0
26	STANDARD		Infinity	0		0	0
27	COORDBRK		-	-0.0001677368		-	-
28	STANDARD	KPC076	-51.65	2.62	BK7	42.92	0
29	STANDARD		Infinity	6.054709		42.92	0
30	COORDBRK		-	0		-	-
31	COORDBRK		-	0		-	-
32	STANDARD	KPX190	Infinity	8.34	BK7	42.92	0
33	STANDARD		-64.64	0		42.92	0
34	COORDBRK		-	300.5519		-	-
35	STANDARD		Infinity	0		0	0
IMA	STANDARD		Infinity			0.03778	0

Table E1